AD-A273 699

:NTATION PAGE

Form Approved
OMB No. 0704-0188

2

1. AGENCY USE ONLY (Leave blank)	2. REPORT DATE	3. REPORT TYPE AND DATES COVERED
	12/93	scientific paper

4. TITLE AND SUBTITLE

Edge Detection using a Complex Wavelet

5. FUNDING NUMBERS

6. AUTHOR(S)

Richard A. Hevenor and Eugene A. Margerum

7. PERFORMING ORGANIZATION NAME(S) AND ADDRESS(ES)

U.S. Army Topographic Engineering Center
ATTN: CETEC-LO
Fort Belvoir, VA 22060-5546

8. PERFORMING ORGANIZATION REPORT NUMBER

R-200

9. SPONSORING/MONITORING AGENCY NAME(S) AND ADDRESS(ES)

10. SPONSORING/MONITORING AGENCY REPORT NUMBER

11. SUPPLEMENTARY NOTES

DEC 15 1993
S B D

12a. DISTRIBUTION/AVAILABILITY STATEMENT

Approved for public release;
distribution is unlimited.

12b. DISTRIBUTION CODE

13. ABSTRACT *(Maximum 200 words)*

A complex wavelet of the form $\psi(x,y) = C(x - jy)e^{-p(x^2+y^2)}$ is used in the continuous wavelet transform to obtain edges from a digital image in two orthogonal directions. In the above equation $\psi(x,y)$ is a two dimensional complex wavelet, C and p are constants, j is the square root of -1 and x and y are position variables. The square root of the sum of the squares of the real and imaginary parts of the wavelet transform are used to find the edges in an arbitrary direction. Theoretical models are derived for the cases of a step edge and a ramp edge. The computer implementation of the wavelet edge detector involves the creation of two masks; one for the real part and one for the imaginary part. An expression is derived for the size of the edge masks using the inflection points of a curve derived from the wavelet. Finally the edge detector is applied to two synthetic aperture radar images and the resulting images are shown.

14. SUBJECT TERMS

continuous wavelet transfor digital image

15. NUMBER OF PAGES

9

16. PRICE CODE

17. SECURITY CLASSIFICATION OF REPORT	18. SECURITY CLASSIFICATION OF THIS PAGE	19. SECURITY CLASSIFICATION OF ABSTRACT	20. LIMITATION OF ABSTRACT
unclassified	unclassified	unclassified	

Edge detection using a complex wavelet

Richard A. Hevenor and Eugene A. Margerum

U. S. Army Topographic Engineering Center
Telegraph and Leaf Roads
Fort Belvoir, Virginia 22060-5546

ABSTRACT

A complex wavelet of the form $\psi(x,y) = C(x - jy)e^{-p(x^2+y^2)}$ is used in the continuous wavelet transform to obtain edges from a digital image in two orthogonal directions. In the above equation $\psi(x,y)$ is a two dimensional complex wavelet, C and p are constants, j is the square root of -1 and x and y are position variables. The square root of the sum of the squares of the real and imaginary parts of the wavelet transform are used to find the edges in an arbitrary direction. Theoretical models are derived for the cases of a step edge and a ramp edge. The computer implementation of the wavelet edge detector involves the creation of two masks; one for the real part and one for the imaginary part. An expression is derived for the size of the edge masks using the inflection points of a curve derived from the wavelet. Finally the edge detector is applied to two synthetic aperture radar images and the resulting images are shown.

1. INTRODUCTION

Edge detection in digital images is a very important operation in computer vision systems. There are a large number of edge detection techniques available, however most of them do not have the capability of detecting edges at different scales. Many of these edge detectors have a small mask size and do not permit points on an edge far away from the point under consideration to be included in the calculations. Such edge detectors would include the Sobel, the Roberts, and the Laplacian. These edge detectors also form finite approximations of differentiation operators and lead to results that are sometimes quite noisy. The purpose of this paper is to present a solution to the above mentioned problems by use of the continuous wavelet transform (CWT) in two dimensions which is given below:

$$W_f(a_x, b_x, a_y, b_y) = \frac{1}{|a_x|^{\frac{1}{2}}|a_y|^{\frac{1}{2}}} \int_{-\infty}^{\infty} \int_{-\infty}^{\infty} f(x,y)\, \overline{\psi\left(\frac{x-b_x}{a_x}, \frac{y-b_y}{a_y}\right)}\, dy\, dx \tag{1}$$

where $W_f(a_x, b_x, a_y, b_y)$ is the wavelet transform of the function $f(x,y)$, $\psi\left(\frac{x-b_x}{a_x}, \frac{y-b_y}{a_y}\right)$ is the wavelet to be chosen depending on the problem to be solved, the horizontal bar over the wavelet in (1) indicates taking the complex conjugate, a_x and a_y are the dilation parameters, and b_x and b_y are the translation parameters. The function $f(x,y)$ will be used to represent an image function such that it will be equal to a specific graytone value at the location given by the coordinates (x,y). It should be noted that we have taken a two dimensional function and transformed it into a four dimensional function. At first this appears to have made the problem much more difficult. The wavelet we use in equation (1) is shown below:

$$\psi(x,y) = C(x - jy)e^{-p(x^2+y^2)} \tag{2}$$

where x and y are position variables, j is the square root of -1, and C and p are constants to be assigned. The one dimensional version of this wavelet is equivalent to a first order Hermite function. The use of Hermite functions as wavelets to be used for edge detection was discussed by Grossmann[1], but he did not develop any specific models or provide any experimental results. This paper is divided into six sections with Section 2 discussing the analytical solution to the step edge problem, Section 3 will discuss edge detection for a ramp edge, Section 4 will derive the wavelet transform in terms of the application of two masks, one for the real part of the transform and one for the imaginary part, also an expression will be derived for the size of the masks, Section 5 will describe some results of applying this wavelet edge detector to two synthetic aperture radar images, and Section 6 will present conclusions. The purpose of sections 2 and 3 is to clearly show the applicability of the chosen wavelet for edge detection.

Typeset by $\mathcal{A}\mathcal{M}\mathcal{S}$-TEX

2. SOLUTION FOR A STEP EDGE

In this section we will derive the equation for the wavelet transform of an image function which consists of only one simple step edge. This step edge can be represented by the following expression for $f(x,y)$:

$$f(x,y)=\begin{cases} A & \text{if } x<0 \\ B & \text{if } x\geq 0 \end{cases} \tag{3}$$

where A and B are image graytones and we take $B>A$. The CWT and the wavelet $\psi(x,y)$ were described in equations (1) and (2). The dilation parameters a_x and a_y will always be positive real numbers. When the wavelet given by (2) is placed in (1) and the CWT is separated into its real and imaginary parts the following result is obtained:

$$\begin{aligned} W_f(a_x,b_x,a_y,b_y) =& \frac{C}{\sqrt{a_x a_y}}\int_{-\infty}^{\infty}\int_{-\infty}^{\infty} f(x,y)\left[\frac{x-b_x}{a_x}\right] e^{-p\left[\left(\frac{x-b_x}{a_x}\right)^2+\left(\frac{y-b_y}{a_y}\right)^2\right]}\,dy\,dx \\ &+\frac{jC}{\sqrt{a_x a_y}}\int_{-\infty}^{\infty}\int_{-\infty}^{\infty} f(x,y)\left[\frac{y-b_y}{a_y}\right] e^{-p\left[\left(\frac{x-b_x}{a_x}\right)^2+\left(\frac{y-b_y}{a_y}\right)^2\right]}\,dy\,dx \end{aligned} \tag{4}$$

Putting the appropriate values for $f(x,y)$ into equation (4) will yield:

$$\begin{aligned} W_f(a_x,b_x,a_y,b_y) =& \frac{C}{\sqrt{a_x a_y}}\int_{-\infty}^{\infty} dy\left\{\int_{-\infty}^{0} A\left(\frac{x-b_x}{a_x}\right) e^{-p\left[\left(\frac{x-b_x}{a_x}\right)^2+\left(\frac{y-b_y}{a_y}\right)^2\right]}\,dx\right. \\ &\left.+\int_{0}^{\infty} B\left(\frac{x-b_x}{a_x}\right) e^{-p\left[\left(\frac{x-b_x}{a_x}\right)^2+\left(\frac{y-b_y}{a_y}\right)^2\right]}\,dx\right\} \\ &+\frac{jC}{\sqrt{a_x a_y}}\int_{-\infty}^{\infty} dy\left\{\int_{-\infty}^{0} A\left(\frac{y-b_y}{a_y}\right) e^{-p\left[\left(\frac{x-b_x}{a_x}\right)^2+\left(\frac{y-b_y}{a_y}\right)^2\right]}\,dx\right. \\ &\left.+\int_{0}^{\infty} B\left(\frac{y-b_y}{a_y}\right) e^{-p\left[\left(\frac{x-b_x}{a_x}\right)^2+\left(\frac{y-b_y}{a_y}\right)^2\right]}\,dx\right\} \end{aligned} \tag{5}$$

Now we let $u=\sqrt{p}\,[(x-b_x)/a_x]$ and $v=\sqrt{p}\,[(y-b_y)/a_y]$. Then $(a_x/\sqrt{p})du=dx$ and $(a_y/\sqrt{p})dv=dy$. Making these substitutions in equation (5) we have:

$$\begin{aligned} W_f(a_x,b_x,a_y,b_y) =& \frac{C}{\sqrt{a_x a_y}}\int_{-\infty}^{\infty}\frac{a_y}{\sqrt{p}}e^{-v^2}\,dv\left\{\int_{-\infty}^{-\frac{b_x\sqrt{p}}{a_x}}\frac{Aa_x u}{p}e^{-u^2}\,du+\int_{-\frac{b_x\sqrt{p}}{a_x}}^{\infty}\frac{Ba_x u}{p}e^{-u^2}\,du\right\} \\ &+\frac{jC}{\sqrt{a_x a_y}}\int_{-\infty}^{\infty}\frac{a_y v}{p}e^{-v^2}\,dv\left\{\int_{-\infty}^{-\frac{b_x\sqrt{p}}{a_x}}\frac{Aa_x}{\sqrt{p}}e^{-u^2}\,du+\int_{-\frac{b_x\sqrt{p}}{a_x}}^{\infty}\frac{Ba_x}{\sqrt{p}}e^{-u^2}\,du\right\} \end{aligned} \tag{6}$$

Because $\int_{-\infty}^{\infty} xe^{-x^2}\,dx=0$, the imaginary part of equation (6) becomes 0. Using the following integrals

$$\int xe^{-x^2}\,dx=-\frac{1}{2}e^{-x^2} \tag{7}$$

$$\int_{-\infty}^{\infty} e^{-x^2}\,dx=\sqrt{\pi} \tag{8}$$

the real part of equation (6) evaluates to:

$$W_f(a_x,b_x,a_y)=\frac{C\sqrt{\pi a_x a_y}\,(B-A)\,e^{-p\left(\frac{b_x}{a_x}\right)^2}}{2p^{\frac{3}{2}}} \tag{9}$$

Equation (9) is the final result for the step edge. It is independent of b_y and when plotted as a function of b_x forms a Gaussian curve with its maximum value centered at the location of the step edge. As the dilation parameter a_x increases, the maximum value of the Gaussian curve increases and the width of the curve also increases. In other words, as a_x increases the edge would appear brighter and thicker. The localization of the step edge for this wavelet, based on the maximum value of equation (9), is exact. In general the wavelet transform will be complex when the step edge is oriented at an arbitrary angle with respect to the x axis and will consist of both a real and an imaginary part:

$$W_f(a_x, b_x, a_y, b_y) = W_{fr}(a_x, b_x, a_y, b_y) + jW_{fi}(a_x, b_x, a_y, b_y) \tag{10}$$

The direction of a unit normal to an edge which points from the smaller graytone to the larger graytone can be computed by taking the inverse tangent of the ratio of the imaginary and real parts of the wavelet transform. If we let θ be the angle between the x axis and the unit normal to the edge, then θ can be found as follows:

$$\theta = \tan^{-1}[W_{fi}(a_x, b_x, a_y, b_y)/W_{fr}(a_x, b_x, a_y, b_y)] + \begin{cases} 0^\circ & \text{if } W_{fr} \text{ is} \geq 0 \\ 180^\circ & \text{if } W_{fr} \text{ is} < 0 \end{cases} \tag{11}$$

The determination of the direction of an edge from its normal can be useful in eliminating edges in certain directions or perhaps in emphasizing edges in certain directions.

3. SOLUTION FOR A RAMP EDGE

In this section we derive an expression for a ramp edge. The ramp edge can be represented mathematically as

$$f(x,y) = \begin{cases} A & \text{if } x \leq 0 \\ qx + b & \text{if } 0 \leq x \leq d \\ B & \text{if } x \geq d \end{cases} \tag{12}$$

The parameter d represents the thickness of the transition zone. At $x = 0$, $f(x,y) = b$; therefore $A = b$. At $x = d$, $f(x,y) = B = qd + A$; therefore $q = (B - A)/d$. The dilation parameters a_x and a_y are positive real numbers. The CWT will take the form shown in equation (1). As in section 2 we let $u = \sqrt{p}(x - b_x)/a_x$ and $v = \sqrt{p}(y - b_y)/a_y$ making $du = (\sqrt{p}/a_x)dx$ and $dv = (\sqrt{p}/a_y)dy$. The imaginary part of the CWT will be equal to 0 as it was in section 2. The integral in u can be separated into three terms as given below:

$$\begin{aligned} W_f(a_x, b_x, a_y, b_y) = \frac{C}{\sqrt{a_x a_y}} \int_{-\infty}^{\infty} \frac{a_y e^{-v^2}}{\sqrt{p}} dv \Bigg\{ & \int_{-\infty}^{-b_x\sqrt{p}/a_x} \frac{A a_x u e^{-u^2}}{p} du \\ & + \int_{-b_x\sqrt{p}/a_x}^{\sqrt{p}(d-b_x)/a_x} \left[q\left(\frac{a_x u}{\sqrt{p}} + b_x\right) + b \right] \frac{a_x u e^{-u^2}}{p} du \\ & + B \int_{\sqrt{p}(d-b_x)/a_x}^{\infty} \frac{a_x u e^{-u^2}}{p} du \Bigg\} \end{aligned} \tag{13}$$

Using techniques similar to those in Section 2 and making use of the definition of the error function [erf(x)]

$$\text{erf}(x) = \frac{2}{\sqrt{\pi}} \int_0^x e^{-t^2} dt \tag{14}$$

the final form of the CWT for a ramp edge becomes:

$$W_f(a_x, b_x, a_y) = \frac{C(B - A)a_x \pi \sqrt{a_x a_y}}{4dp^2} [\text{erf}(h) - \text{erf}(k)] \tag{15}$$

where $h = \sqrt{p}[(d - b_x)/a_x]$ and $k = -b_x\sqrt{p}/a_x$. This equation is independent of b_y and when plotted as a function of b_x will form a curve where the peak is located in the center of the linear transition zone. Only one edge is found and its brightness and width depends upon the value for a_x just as it did for the step edge problem in Section 2. When a_x increases the peak value of the curve increases but so does its width.

4. DERIVATION OF THE WAVELET TRANSFORM MASKS

The computer implementation of the wavelet edge detector involves the creation of two masks; one for the real part of the wavelet transform and one for the imaginary part. The numerical values that are placed in each of the masks can be computed from the discrete approximation of the wavelet transform, $\hat{W}_f(a_x, b_x, a_y, b_y)$:

$$\hat{W}_f(a_x, b_x, a_y, b_y) = \frac{1}{\sqrt{a_x a_y}} \sum_{m=b_x-\frac{(L-1)}{2}}^{b_x+\frac{(L-1)}{2}} \sum_{n=b_y-\frac{(L-1)}{2}}^{b_y+\frac{(L-1)}{2}} f(m,n) \left[\psi_r\left(\frac{m-b_x}{a_x}, \frac{n-b_y}{a_y}\right) + j\psi_i\left(\frac{m-b_x}{a_x}, \frac{n-b_y}{a_y}\right)\right] \tag{16}$$

where:

$$\psi_r\left(\frac{m-b_x}{a_x}, \frac{n-b_y}{a_y}\right) = C\left[\frac{m-b_x}{a_x}\right] e^{-p\left[\left(\frac{m-b_x}{a_x}\right)^2+\left(\frac{n-b_y}{a_y}\right)^2\right]} \tag{17}$$

$$\psi_i\left(\frac{m-b_x}{a_x}, \frac{n-b_y}{a_y}\right) = C\left[\frac{n-b_y}{a_y}\right] e^{-p\left[\left(\frac{m-b_x}{a_x}\right)^2+\left(\frac{n-b_y}{a_y}\right)^2\right]} \tag{18}$$

It will be assumed that each mask is a square with L rows and L columns. Requiring that L be an odd number, we let $r = m - b_x + 1 + (L-1)/2$ and let $s = n - b_y + 1 + (L-1)/2$. Equation (16) can then be rewritten as:

$$\begin{aligned}\hat{W}_f(a_x, b_x, a_y, b_y) = \frac{1}{\sqrt{a_x a_y}} \sum_{r=1}^{L}\sum_{s=1}^{L} f(r + b_x - 1 - (L-1)/2,\, s + b_y - 1 - (L-1)/2) \cdot \\ \left[\psi_r\left(\frac{r-1-(L-1)/2}{a_x}, \frac{s-1-(L-1)/2}{a_y}\right)\right. \\ \left. +j\psi_i\left(\frac{r-1-(L-1)/2}{a_x}, \frac{s-1-(L-1)/2}{a_y}\right)\right]\end{aligned} \tag{19}$$

The two masks $M_r(r,s)$ and $M_i(r,s)$ can now be written as:

$$M_r(r,s) = \frac{C}{\sqrt{a_x a_y}}\left[\frac{r-1-(L-1)/2}{a_x}\right] e^{-p\left[\left(\frac{r-1-(L-1)/2}{a_x}\right)^2+\left(\frac{s-1-(L-1)/2}{a_y}\right)^2\right]} \tag{20}$$

$$M_i(r,s) = \frac{C}{\sqrt{a_x a_y}}\left[\frac{s-1-(L-1)/2}{a_y}\right] e^{-p\left[\left(\frac{r-1-(L-1)/2}{a_x}\right)^2+\left(\frac{s-1-(L-1)/2}{a_y}\right)^2\right]} \tag{21}$$

In the above two equations both r and s vary from 1 to L. It can be seen that the values placed in the masks are functions of the dilation parameters a_x and a_y so that the masks must be recomputed each time there is a change in one or both of the dilation parameters. The values placed in the two masks must also be recomputed if one or both of the constants p and C are changed or if the size of the masks is changed. If we let H_r be the result of applying the mask $M_r(r,s)$ to an image at a particular point, say (x,y), and we let H_i be the result of applying the mask $M_i(r,s)$ at the same point, then the final computation for the magnitude of an edge at this point will be $H[f(x,y)]$ and is given below:

$$H[f(x,y)] = [H_r^2 + H_i^2]^{1/2} \tag{22}$$

The direction of the normal to the edge at the point (x,y) and measured with respect to the x axis can be represented by $\theta(x,y)$ and can be computed as:

$$\theta(x,y) = \tan^{-1}(H_i/H_r) + \begin{cases} 0^\circ & \text{if } H_r \text{ is } \geq 0 \\ 180^\circ & \text{if } H_r \text{ is } < 0 \end{cases} \tag{23}$$

The only other thing which needs to be derived is an expression for the size L of the masks themselves. This will be done by making use of the location of the inflection points of a curve that can be found from the wavelet. The wavelet itself can be divided into real and imaginary parts:

$$\psi(x,y) = \psi_r(x,y) - j\psi_i(x,y) \tag{24}$$

Letting $h(x,y) = \psi\left(\frac{x-b_x}{a_x}, \frac{y-b_y}{a_y}\right)$ then $h(x,y)$ can also be divided into real and imaginary parts [$h_r(x,y)$ and $h_i(x,y)$]:

$$h(x,y) = h_r(x,y) - jh_i(x,y) \tag{25}$$

In solving for L we will let a_x, b_x, y, a_y, and b_y, be constants and consider the curve which is formed in the $h_r(x,y)$ and x plane. This curve will have inflection points, two of which are close to the x axis and the distance between them can be used in determining a value for L. Letting $u = (x - b_x)/a_x$ and $v = (y - b_y)/a_y$ and differentiating $h_r(x,y)$ with respect to x will yield:

$$\frac{\partial h_r}{\partial x} = \frac{C}{a_x}[1 - 2pu^2]e^{-p(u^2+v^2)} \tag{26}$$

Differentiating $h_r(x,y)$ a second time with respect to x will give:

$$\frac{\partial^2 h_r}{\partial x^2} = -\frac{2C}{a_x^2}[2pu + (1 - 2pu^2)pu]e^{-p(u^2+v^2)} \tag{27}$$

An inflection point is found by simply setting 27 equal to zero:

$$2pu + (1 - 2pu^2)pu = 0 \tag{28}$$

One solution to (28) is $u = 0$. If u is not zero then the following solution is obtained:

$$u = \pm\sqrt{\frac{3}{2p}} \tag{29}$$

Since $u = (x - b_x)/a_x$ we have for x:

$$x = b_x \pm a_x\sqrt{\frac{3}{2p}} \tag{30}$$

A similar result can be obtained for y by setting $\frac{\partial^2 h_i}{\partial y^2} = 0$:

$$y = b_y \pm a_y\sqrt{\frac{3}{2p}} \tag{31}$$

The distance between the two inflection points which are the furthest away from each other and located along the x-axis will be $2a_x\sqrt{3/(2p)}$. Along the y-axis the distance between these inflection points will be $2a_y\sqrt{3/(2p)}$. The mask size must be large enough to cover the larger of these two distances in order to include the area where the wavelet would still have a significant finite value. Doubling the larger of these two distances would insure that the masks cover an area outside of which the wavelet has an insignificant value. The value for L must be odd since it will be necessary to calculate edges for an image pixel at the center of the masks. The absolute minimum mask size will be 3 x 3 although in general much larger mask sizes will yield better results. Given the above constraints, one of the following six expressions will allow a value for L to be determined and the operator (int) means to round off to the nearest integer:

1. $L = (\text{int})[4a_x\sqrt{3/(2p)}]$ if $a_x \geq a_y$ and $(\text{int})[4a_x\sqrt{3/(2p)}]$ is odd and ≥ 3
2. $L = (\text{int})[4a_x\sqrt{3/(2p)}] + 1$ if $a_x \geq a_y$ and $(\text{int})[4a_x\sqrt{3/(2p)}]$ is even and ≥ 2
3. $L = (\text{int})[4a_y\sqrt{3/(2p)}]$ if $a_y > a_x$ and $(\text{int})[4a_y\sqrt{3/(2p)}]$ is odd and ≥ 3
4. $L = (\text{int})[4a_y\sqrt{3/(2p)}] + 1$ if $a_y > a_x$ and $(\text{int})[4a_y\sqrt{3/(2p)}]$ is even and ≥ 2

5. $L = 3$ if $a_x \geq a_y$ and (int)$[4a_x\sqrt{3/(2p)}] < 2$
6. $L = 3$ if $a_y > a_x$ and (int)$[4a_y\sqrt{3/(2p)}] < 2$.

5. APPLICATION OF THE WAVELET EDGE DETECTOR TO SYNTHETIC APERTURE RADAR IMAGES

The purpose of this section is to show some results of applying the wavelet edge detector to two synthetic aperture radar images. Each image consists of 512 by 512 pixels and has 256 gray levels (0 to 255). The following list of image processing algorithms was used on the original images:

1. Speckle Reduction using a Geometric Filter
2. Edge Preserving Smoothing
3. Edge Detection using the Wavelet Transform
4. Thresholding
5. Thinning
6. Elimination of Small Connected Components
7. Connected Components
8. Outermost Borders
9. Eliminate Pixels not on the Outermost Borders

When performing edge detection on radar imagery one seldom applies an edge operator directly to the original image. This is because synthetic aperture radar imagery contains speckle noise which is very annoying to both human interpreters and to computer vision algorithms. A geometric filter[2] was used to reduce speckle noise. The purpose of the edge preserving smoothing algorithm is to eliminate noise and at the same time preserve edges from degradation. The variation of the gray tone in a neighborhood around each pixel is used to determine the direction that is most homogeneous. Smoothing is then performed in this direction. The specific scheme used for edge preserving smoothing was developed by Nagao and Matsuyama[3]. Edge detection is performed using the CWT as described above. The following values were used for the constants C, p, a_x, and a_y:

$$p = 1$$
$$a_x = 2$$
$$a_y = 2$$
$$C = 255(2)p^{3/2}/[\sqrt{\pi a_x a_y}w]$$

where w is the smallest gray level difference for which an edge will be required. For the images discussed in this section w was set equal to a value of 30. The above expression for C comes from the solution to the step edge problem which was given in section 2. Step edges which have a gray level difference of w or greater will end up with the maximum gray value of 255. Step edges which have a gray level difference less than w will be set to a gray level less than 255. This allows edges with small gray level differences to easily be eliminated by a simple thresholding operation where the threshold is set equal to 254. The value of L (mask size) which corresponds with the above parameter values is 11. A thinning operation is then required in order to thin most edges down to the thickness of 1 pixel in width. Short edges and components are then eliminated. The purpose of the connected components routine is to provide a unique label for each component of 1-pixels in the binary image that has been thinned. Each label is a number that is assigned to every pixel in a given connected component. Use was made of the definition of 8-connectivity for 1-pixels and 4-connectivity for 0-pixels. These definitions were also used for the thinning operation. An algorithm which finds the outermost borders is then utilized. Border following determines and uniquely labels all 1-pixels that exist between a given connected component of 1-pixels and a connected component of 0-pixels. A border point is defined as a 1-pixel that has at least one 0-pixel in its 4-neighborhood. There are two types of borders, hole borders and outer borders. Outermost borders are outer borders which are not surrounded by any other outer borders. The particular border following routine used here was developed by Suzuki and Abe[4]. The last image processing algorithm utilized is that of eliminating all of the pixels which are not on an outermost border. This is a simple operation because when a pixel is found to be on an outermost border it is given a unique label (255). Therefore all pixels which do not have this label are set to zero.

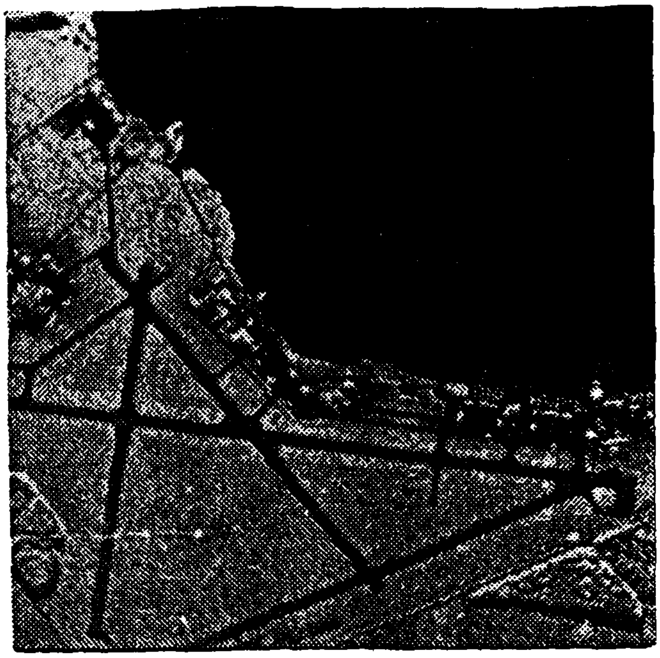

Figure 1: Original Radar Image of an Airfield

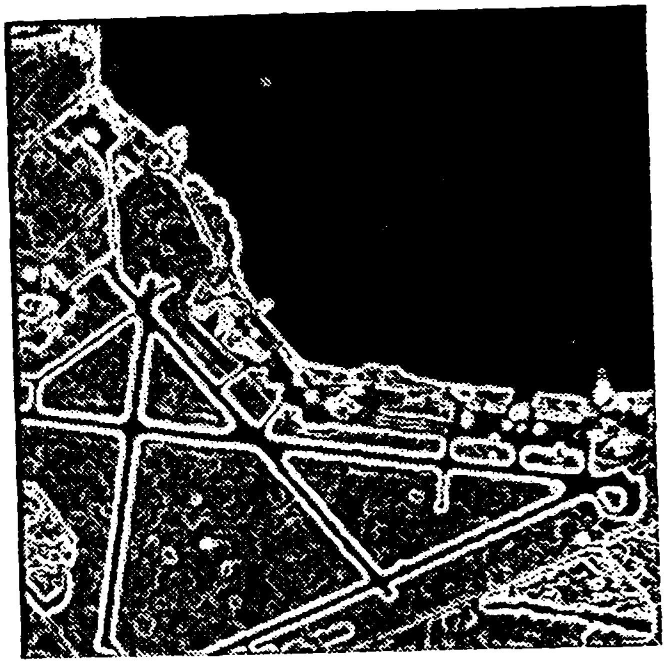

Figure 2: Radar Image of Airfield after Edge Detection

Figure 1 shows a synthetic aperture radar image of an airfield located near Elizabeth City, North Carolina. The image is 512 by 512 pixels and was digitized with 8 bits. The radar system used to obtain this image was the UPD-4 system which is an X-band radar with HH polarization. Figure 2 shows the resulting image after edge detection using the CWT. The edges defining the runways are clearly visible. However, many edges located between runways can be seen which do not correspond with any significant terrain feature. These edges can easily be eliminated by the simple thresholding operation mentioned above. Figure 3 shows the final result after the elimination of pixels

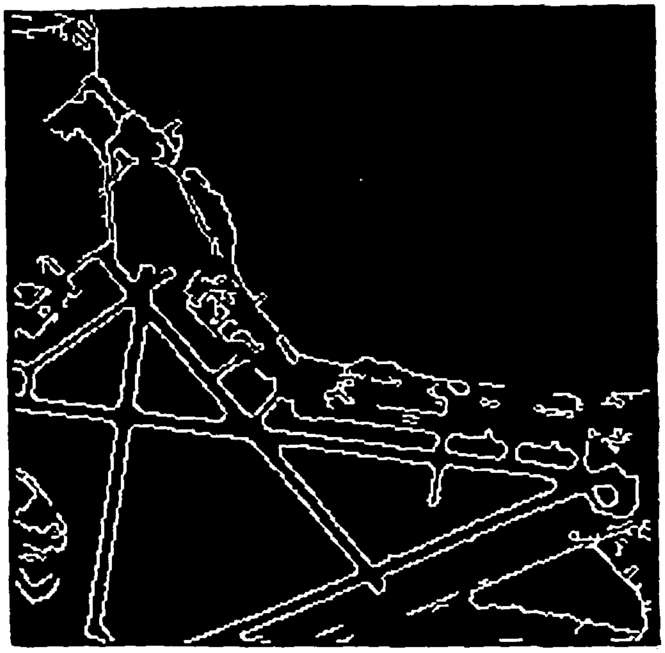

Figure 3: Radar Image of Airfield After Elimination of Pixels Not on the Outermost Borders

Figure 4: Original Radar Image of a River Area

which are not on an outermost border. The edges of the runway pattern are clearly defined and have been thinned. Also there are almost no edges between runways. Figure 4 shows another synthetic aperture radar image of a river located near Elizabeth City, North Carolina. This image is also 512 by 512 pixels and was digitized with 8 bits. The radar system used to obtain this image was also the UPD-4. Figure 5 shows the final result after all nine image processing algorithms were applied to the image shown in Figure 4. The edges defining the boundaries of the river

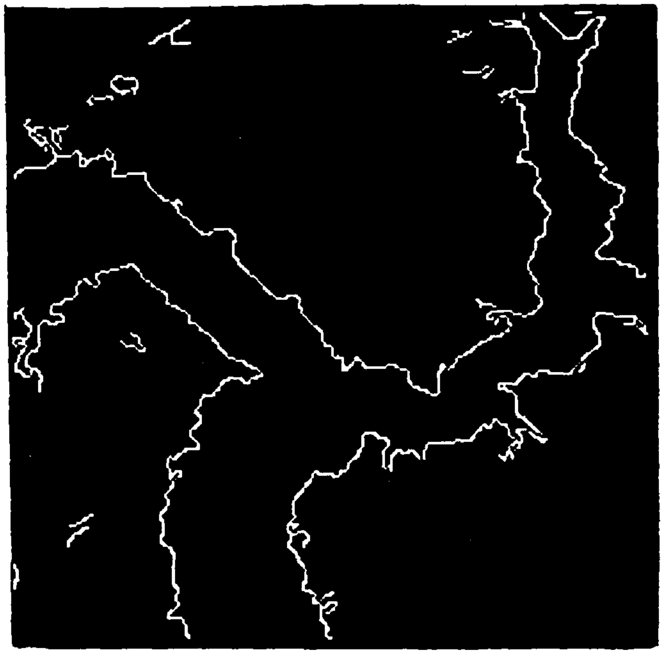

Figure 5: Radar Image of River Area After Elimination of Pixels Not on the Outermost Borders

are clearly seen while other edges have been eliminated.

6. CONCLUSION

The edge detector developed in this paper using the stated complex wavelet, is a very powerful approach to the problem of edge detection. The theory for both a simple step edge and a ramp edge show that the edge detector has only one peak which occurs exactly where the edge should be. Also, good results were shown for some actual radar images.

7. REFERENCES

1. A. Grossman, "Wavelet Transforms and Edge Detection", in Stochastic Processes in Physics and Engineering, S. Albeverio et al., Eds., pp. 149-157, D. Reidel, Dordrecht, the Netherlands, 1988.

2. Thomas R. Crimmins, "Geometric Speckle Reduction", Final Report, AD-A174 628, Environmental Research Institute of Michigan, October, 1896.

3. M. Nagao and T. Matsuyama, A Structural Analysis of Complex Aerial Photographs, Plenum Press, New York, 1980.

4. S. Suzuki and K. Abe, "Topological Structural Analysis of Digitized Binary Images by Border Following", Computer Vision, Graphics and Image Processing, No. 30, pp. 32-46, 1885.